ELSEVIER

Carbon nanomaterials for high-performance supercapacitors

Tao Chen and Liming Dai*

Center of Advanced Science and Engineering for Carbon (Case4Carbon), Department of Macromolecular Science and Engineering, Case Western Reserve University, 10900 Euclid Avenue, Cleveland, OH 44106, USA

Owing to their high energy density and power density, supercapacitors exhibit great potential as high-performance energy sources for advanced technologies. Recently, carbon nanomaterials (especially, carbon nanotubes and graphene) have been widely investigated as effective electrodes in supercapacitors due to their high specific surface area, excellent electrical and mechanical properties. This article summarizes the recent progresses on the development of high-performance supercapacitors based on carbon nanomaterials and provides various rational concepts for materials engineering to improve the device performance for a large variety of potential applications, ranging from consumer electronics through wearable optoelectronics to hybrid electric vehicles.

Introduction

Global energy consumption, along with CO_2 emission, has been accelerating at an alarming rate due to rapid global economic expansion, an increase in the world population, and an ever-increasing human reliance on energy-consuming appliances. It has been estimated that the world will need to double its energy supply by 2050 (see the World Energy Council Website at www.worldenergy.org). The rapid increase in global energy consumption and the environmental impact of traditional energy resources pose serious challenges to human health, energy security, and the environment; and reveal a growing need to develop new types of clean and sustainable energy conversion and storage systems, such as batteries and supercapacitors for electric vehicles with low exhaust emissions.

Supercapacitors, also called as ultracapacitors, are electrochemical energy storage devices that combine the high energy-storage-capability of conventional batteries with the high power-delivery-capability of conventional capacitors [1–4]. Being able to achieve higher power and longer cycle life than conventional dielectric capacitors and batteries, supercapacitors have been developed to provide power pulses for a large variety of applications, ranging from consumer electronics through hybrid electric vehicles (HEVs) to industrial electric utilities [5]. Therefore, supercapacitors play an important role in achieving better fuel economy, decreasing harmful emissions, and reducing the reliance on petroleum sources. The world market for supercapacitors has been growing steadily and rapidly [1]. To improve the performance of state-of-the-art supercapacitors to meet the stringent requirements for the applications mentioned above, and many other advanced applications not discussed (e.g. portable, transparent and wearable electronics), new electrode materials with superior properties over those of current activated carbon electrodes are needed and new device structures (e.g. all-solid state supercapacitors [6,7], optically transparent [8,9], mechanically flexible and stretchable [10–12], and even fiber-shaped [13–15] supercapacitors) are highly desirable.

Nanotechnology has opened up new frontiers by offering unique enabling technologies and new materials for energy storage. In particular, graphitic carbon nanomaterials (e.g. carbon nanotubes, graphene sheets) have been playing a more and more important role in the development of high-performance supercapacitors [4,5]. The aim of this article is to summarize recent progress in the development of supercapacitors (especially electrical double layer capacitors) based on carbon nanomaterials and to provide various rational concepts for materials engineering to improve device performance.

Supercapacitors

A typical supercapacitor consists of three essential components, namely the electrodes, the electrolyte, and the separator. The overall performance of supercapacitors is determined by the

*Corresponding author:. Dai, L. (liming.dai@case.edu)

 1369-7021/06/$ - see front matter http://dx.doi.org/10.1016/j.mattod.2013.07.002

physical properties of both the electrode and the electrolyte materials. Nevertheless, the electrode is one of the most important components for charge storage/delivery, and plays a crucial role in determining the energy and power densities of a supercapacitor. The electrochemical performance of a supercapaictor can be characterized by cyclic voltammetry and galvanostatic charge–discharge measurements [1–4]. The capacitance (C) is determined from the constant current discharge curves according to Eqn 1:

$$C = \frac{I}{(dV/dt)} \tag{1}$$

where I is the discharge current and dV/dt is calculated from the slope of the discharge curve. Then, the specific capacitance (C_{SP}) for one electrode in a supercapacitor can be calculated using the following equation:

$$C_{SP}\,(\mathrm{F\ g^{-1}}) = \frac{4C}{m} \tag{2}$$

where C is the measured capacitance for the two-electrode cell and m is the total mass of the active materials in both electrodes. The mass can also be replaced by volume or area of the electrodes depending on the nature of the targeted applications. The stored energy (E) and the power density (P) in a supercapacitor can then be calculated from Eqns 3 and 4, respectively:

$$E = \frac{(CV^2)}{2} \tag{3}$$

$$P = \frac{V^2}{(4R_s)} \tag{4}$$

where C ($\mathrm{F\ g^{-1}}$) is the total capacitance of the cell, V is the cell voltage, and R_S is the equivalent series resistance.

The principle of energy storage in a supercapacitor can be either (i) electrostatic charge accumulation at the electrode/electrolyte interface (electrical double layer capacitance, EDLC), as schematically shown in Fig. 1, or (ii) charge transfer, via reversible (Faradaic) redox reaction(s), to redox materials (e.g. conductive polymers, metal oxide nanoparticles) on the surface of electrode (pseudo-capacitance). In practical supercapacitors, the two storage mechanisms often work simultaneously [16]. Different charge transfer processes involved in the EDLC and pseudo-capacitance [4,5,16]. In EDLC, the energy is stored through ion adsorption (a purely electrostatic process) at the electrode-electrolyte interface with no charge transfer across the electrodes, suggesting a non-faradic process. By contrast, pseudo-capacitance arises from reversible redox reaction(s) between the electrolyte and active species on the surface of electrodes. Although pseudo-capacitance higher than EDLC capacitance can be achieved, supercapacitors based on pseudo-capacitance often suffer from the poor electrical conductivity of the electroactive species, and hence demonstrate low power density and cycling stability. Therefore, the combination of both EDLC and pseudo-capacitance presents an effective means to improve the overall capacitance of a supercapacitor.

Since both EDLC and pseudocapacitance are surface phenomena, high-surface-area mesoporous carbon and activated carbons (specific surface area: 1000–2000 $\mathrm{m^2\ g^{-1}}$) have been widely used as electrode materials in both academic and commercial supercapacitors [16–19]. Taking a specific surface area of 1000 $\mathrm{m^2\ g^{-1}}$ for carbon as an example, its ideal attainable capacitance could be 200–500 $\mathrm{F\ g^{-1}}$. However, the practically obtained values are of only a few tens of $\mathrm{F\ g^{-1}}$. Activated carbons have a wide pore size distribution, consisting of micropores (<2 nm), mesopores (2–50 nm), and macropores (>50 nm) [17,18], with most of the surface area of activated carbons being on the scale of micropores [20]. Pores of this size are often poorly or non-accessible for electrolyte ions (especially for organic electrolytes), and thus are incapable of supporting an electrical double layer. By contrast, mesopores contribute the most to the capacitance in an electrical double-layer capacitor [21–23]. However, recent experimental and theoretical studies have demonstrated that charge storage in pores 0.5–2 nm in size (smaller than the size of solvated electrolyte ions) increased with decreasing pore size due to the closer approach of the ion center to the electrode surface in the smaller pores [18,24–26]. Pores less than 0.5 nm wide are too small for double layer formation [26]. Currently available activated carbon materials have a high surface area but unfortunately a low mesoporosity, and hence a limited capacitance due to a low electrolyte accessibility [20]. This translates to the limited energy density of the resultant supercapacitors (Eqn 3). The low electrolyte accessibility of activated carbons, coupled with their poor electrical conductivity, produces a high internal resistance and hence a low power density for the capacitors (Eqn 4) [20]. Consequently, a limited energy density (4–5 $\mathrm{Wh\ kg^{-1}}$) and a limited power density

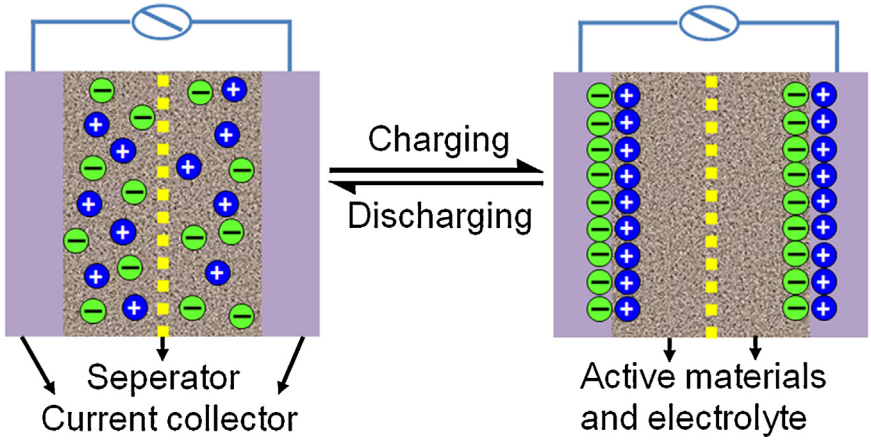

FIGURE 1

Schematic illustration of the charging/discharging process in a supercapacitor.

(1–2 kW kg^{-1}) have been obtained for currently available supercapacitors based on the activated carbon electrodes [20]. Clearly, therefore, new materials are needed to overcome the drawbacks of activated carbon electrode materials to improve the performances for supercapacitors.

Owing to their large surface area, high mesoporosity and electrolyte accessibility, and good electrical properties, carbon nanomaterials, especially graphene and carbon nanotubes (CNTs), are very promising candidates to replace activated carbons as the electrode materials in high-performance supercapacitors [27,28]. Graphene, a single-atom-thick layer of sp^2 carbon atoms densely packed into a two-dimensional (2D) honeycomb lattice, can be viewed as the basic building block for carbon materials of all other dimensionalities, such as 0D fullerene, 1D nanotubes, and 3D graphite (Fig. 2) [27]. For instance, a carbon nanotube (CNT) may be conceptually viewed as a graphene sheet that is rolled into a nanoscale tube form as a single-walled carbon nanotube (SWNT), or as a multiwalled carbon nanotube (MWNT) with additional graphene coaxial tubes around the SWNT core [29].

CNTs with a high aspect ratio, large specific surface area (SWNT >1600 $m^2 g^{-1}$, MWNT >430 $m^2 g^{-1}$) [30,31] as well as good mechanical and electrical (~5000 S cm^{-1}) properties have been widely used as the active electrodes in supercapacitors [28,32–37]. Having many similarities to CNTs in structure and properties, including its high aspect ratio (the ratio of lateral size to thickness), large surface (2630 $m^2 g^{-1}$) [38–40], excellent carrier mobility (15,000 $cm^2 V^{-1} s^{-1}$ for both electrons and holes) [41], and good mechanical properties [42], graphene is an attractive candidate for many potential applications where CNTs have been exploited. Superior to CNTs, one-atom-thick graphene sheets with a 2D planar geometry could offer additional advantages as more effective electrode materials in supercapacitors [43]. Furthermore, the availability of many rational strategies for materials engineering and rich chemistries for controlled functionalization of both CNTs and graphene should facilitate materials engineering for the development of various high-performance supercapacitors based on carbon nanomaterials, as described below.

High-performance supercapacitors by controlling the orientation and tip structure of carbon nanotubes

As mentioned above, CNTs with a high aspect ratio, large specific surface area [30,31] and high electrical conductivity have been widely used as the active electrode in supercapacitors [28,32–37]. For instance, a supercapacitor of a specific capacitance of 102 F g^{-1} with a power density >8 kW kg^{-1} and an energy density of ~1 Wh kg^{-1} has been fabricated from electrodes based on free-standing mats of entangled MWNTs in H_2SO_4 electrolyte [31]. More recently, a higher specific capacitance of 180 F g^{-1} has been

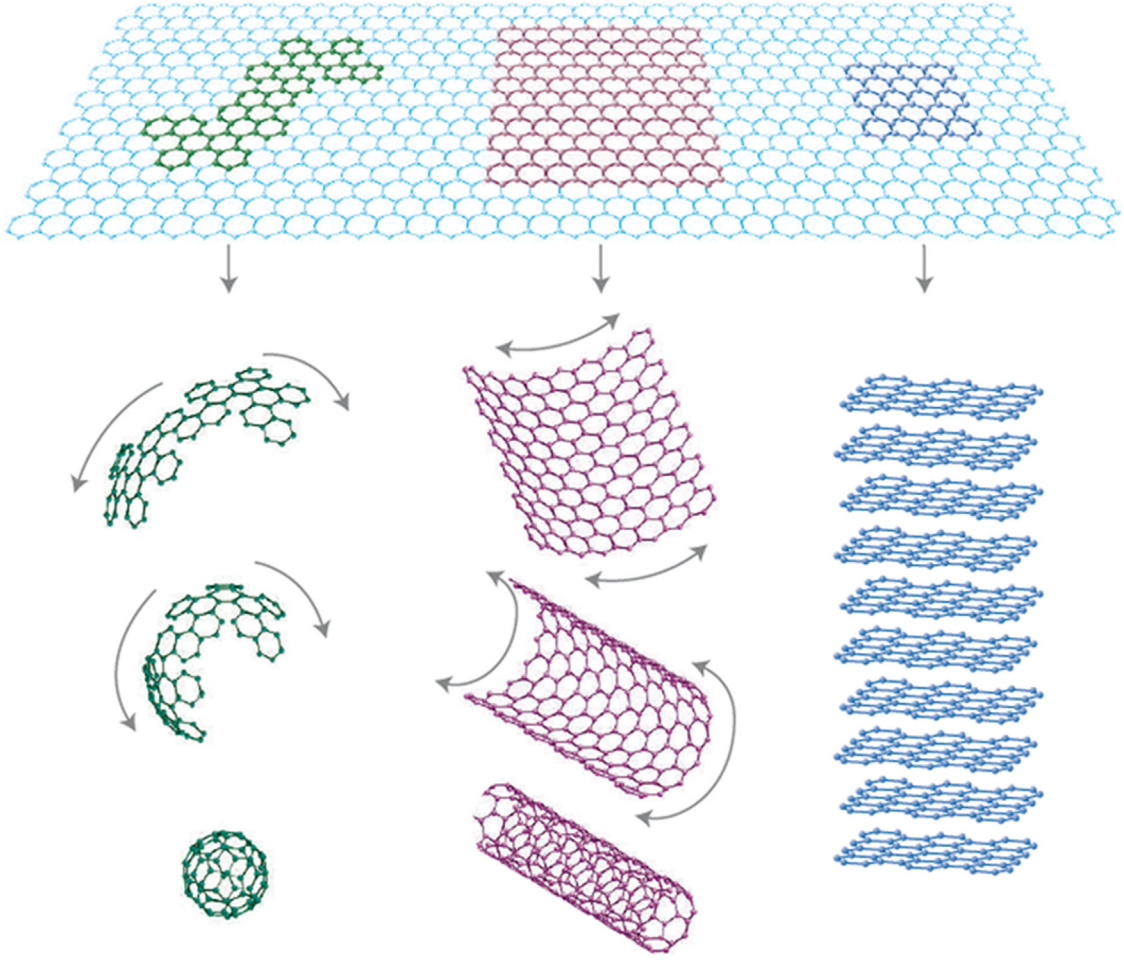

FIGURE 2

The mother of all graphitic forms. Graphene is a 2D building block for carbon materials of all other dimensionalities. It can be wrapped up into 0D buckyballs, rolled into 1D nanotubes or stacked into 3D graphite [27]. Reprinted from Ref. [27] with permission. Copyright 2007, Nature Publishing Group.

achieved when a random SWNT network (Fig. 3a) was used as the electrode in a KOH electrolyte [32]. In this particular case, the maximum power density and energy density approached 20 kW kg^{-1} and 10 Wh kg^{-1}, respectively. This value of power density is higher than those attainable by activated carbon-based commercial capacitors, but the energy density still needs to be improved. The randomly entangled or bundled structure could have significantly reduced the CNT specific area with a concomitant decrease in the electrochemical energy-storage performance [35,44,45].

Compared to their randomly entangled counterparts, vertically-aligned CNT arrays (VA-CNTs) have been demonstrated to be advantageous for supercapacitor applications. Unlike the irregular pore structures of random CNTs (Fig. 3a), the vertically-aligned structure and the well-defined tube-spacing in a VA-CNT array (Fig. 3b,c) can provide a more electrolyte-accessible surface. The aligned structures should also provide improved charge storage/delivery properties as each of the constituent aligned tubes can be connected directly onto a common electrode to allow them to effectively participate in the charging/discharging process (Fig. 3d). Moreover, the top end-caps of the VA-CNTs can be properly opened (e.g. by plasma etching [44,46]) (Fig. 3e–g) to allow the electrolyte access to the otherwise inaccessible inner cavity of the VA-CNTs for charge storage. Indeed, recent research has demonstrated the improved rate capability of VA-CNTs over randomly entangled CNTs [35,44–49], along with enhanced energy density (148 Wh kg^{-1}) and power density (315 kW kg^{-1}) [50–55]. Specifically, a high capacitance has been obtained in 1 M H_2SO_4 for a VA-CNT array electrode (365 F g^{-1}) prepared by template-assisted CVD [56] and in ionic liquid electrolytes [57] for an VA-CNT electrode (440 F g^{-1}) prepared by a template-free CVD approach (Fig. 3e–h) [44,49]. To further optimize the performance of VA-CNT supercapacitors, conductive polymer (e.g. polyaniline [58] and polypyrrole [59]) and metal oxide (e.g. MnO_2 [60], TiO_2 [61] and RuO_2 [62]) can be deposited onto the surface of CNTs to introduce pseudocapacitance.

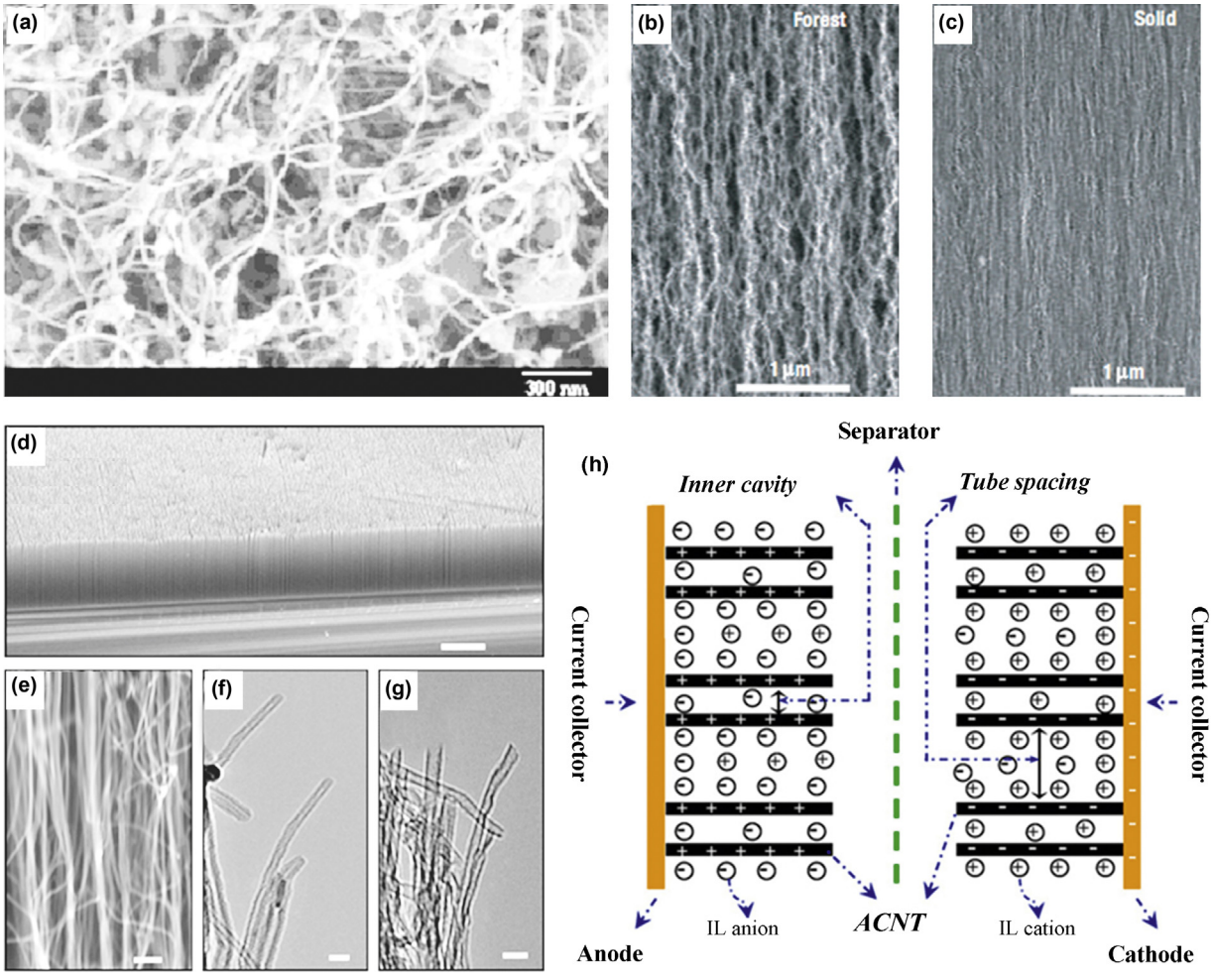

FIGURE 3

Typical structures of random, VA-CNTs and the schematic illumination of VA-CNT based supercapacitors. (a) SEM image of the as -grown randomly entangled SWNTs [32]. Reprinted from Ref. [32] with permission. Copyright 2001, John Wiley and Sons. (b,c) SEM images of the as-grown forest (b) after having been solidified with a droplet of liquid (c) [35]. Reprinted from Ref. [35] with permission. Copyright 2006, Nature Publishing Group. (d) SEM image of a plasma-etched VA-CNT electrode (scale bar: 100 μm). (e) Higher magnification view of the electrode (scale bar: 100 nm). TEM images of the CNTs before (f) and after (g) plasma etching (scale bar: 20 nm) (h) Schematic of an electrochemical capacitor based on plasma-etched VA-CNT electrodes and ionic liquid electrolyte. [44]. Reprinted from Ref. [44] with permission. Copyright 2009, Elsevier.

High-performance supercapacitors by controlling the edge-structure and π–π stacking of graphene sheets

Supercapacitors based on CNT electrodes do not exhibit the expected performance (e.g. specific capacitance below 500 F g^{-1}) due to the high contact resistance between the CNT electrode and current collector and its inefficient interaction with the electrolyte. Besides, it is difficult, if not impossible, to scale up the production of VA-CNTs for the commercialization of supercapacitors [63]. The recent availability of solution-processable graphene oxide (GO) by exfoliation of graphite powder via solution oxidation [64] and edge-functionalized graphene (EFG) sheets via ball milling [65,66] has allowed for the large-scale production of graphene materials at a relatively low cost for various device applications through solution processing [67]. Due to its large surface area, high carrier transport mobility and excellent thermal/mechanical stability, graphene has recently been studied as an alternative carbon based electrode in supercapacitors [68]. Theoretically, the double-layer capacitance value of a graphene electrode can reach up to 550 F g^{-1}, the highest value of intrinsic capacitance among all carbon-based electrodes [69,70]. Using chemically reduced graphene oxide electrodes, a supercapacitor with specific capacitances of 135 and 99 F g^{-1} in aqueous and organic electrolytes, respectively, has been fabricated [39], as was a supercapacitor with ultrahigh specific energy density (85.6 Wh kg^{-1} at room temperature and 136 Wh kg^{-1} at 80 °C) [70]. Recently, supercapacitors with high specific capacitance (276 F g^{-1}), power density (20 W cm^{-3}, 20 times higher than that of the activated carbon counterpart), energy density (1.36 mWh cm^{-3}, 2 times higher than that of the activated carbon counterpart), and excellent stability during bending from 0° to 180° have also been developed by using a standard LightScribe DVD optical drive to directly reduce graphene oxide films to graphene electrodes (Fig. 4a–c) [71]. The performance can be further enhanced by using a conductive polymer [72,73] or metal oxide [74,75] coating to introduce pseudocapacitance.

Recent work on the EFG with various edge groups (e.g. –H, –COOH and $–SO_3H$) by effective and eco-friendly ball milling of graphite (Fig. 4d) provides an effective means for the development of functionalized graphene materials with tailor-made chemical structures and electronic properties attractive for multifunctional applications [65], including large-area transparent and conducting electrodes for electronics and metal-free catalysts for oxygen reduction reaction in fuel cells [66]. Although EFGs have hardly been exploited for energy-storage application, the use of EFGs, having abundant active sites at the edge and perfect conjugation (conductivity) on its basal plane, as the electrode materials could lead to high-performance supercapacitors with a high rate capability. Through controllable self-assembling, EFGs should also facilitate the formation of hierarchically structured electrodes in supercapacitors for specific applications.

High-performance supercapacitors based on 3D pillared graphene-carbon nanotube networks

Although graphene sheets with a large surface area are ideal electrode materials for energy storage, a large portion of the surface

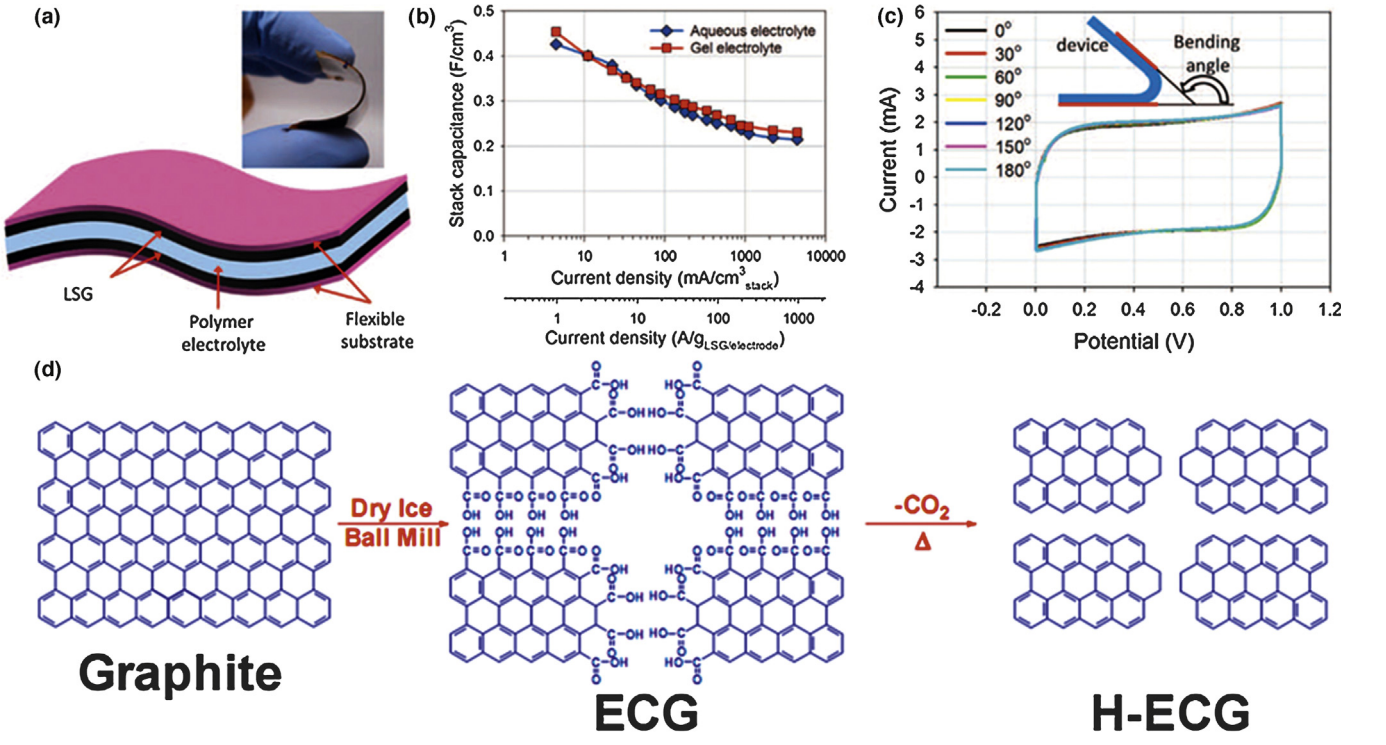

FIGURE 4

Structure and electrochemical properties of an all-solid-state supercapacitor based on laser-scribed graphene (LSG) and the synthetic route to edge-functionalized graphene. (a) Schematic diagram of the supercapacitor based on LSG. Inset is a photograph showing the flexibility of the device. (b) A comparison between performances of LSG-EC using gelled versus aqueous electrolytes. (c) Flexibility of the LSG-based supercapacitor: current–voltage measurements were collected at a scan rate of 1000 mV s^{-1} [71]. Reprinted from Ref. [71] with permission. Copyright 2012, AAAS. (d) Syntheses and proposed structures of edge-carboxylated graphene (ECG) and heat-treated (decarboxylated) ECG (H-ECG) [65]. Reprinted from Ref. [65] with permission. Copyright 2012, the National Academy of Sciences.

area associated with individual graphene sheets in the graphene electrode is inaccessible due to restacking via the strong π–π interaction. Therefore, it is crucial to physically separate 2D graphene sheets to preserve their high surface area, for example by template-assisted construction of 3D graphene foams (Fig. 5a,b) with a porous structure and large surface area [76–79]. In addition, a solution layer-by-layer self-assembling approach to prepare multilayered hybrid carbon films of alternating poly(ethyleneimine)-modified graphene sheets and acid-oxidized MWNT layers was developed to construct supercapacitors with a relatively high specific capacitance of 120 F g^{-1} (higher than those of vertically-aligned [35] and random CNT electrodes [32]) and rate capability since the well-defined interlayers of CNT networks allowed for not only a fast ion diffusion but also efficient electron transport [80]. However, it is difficult to control the porosity and pore distribution within the multilayered CNT/graphene hybrid film as each of the constituent CNT and graphene layers is randomly assembled, and hence it is infeasible to further improve the device performance. To address this issue, 3D pillared VA-CNT/graphene architectures with alternating VA-CNT and graphene layers, whose porous structure and pore distribution can be easily controlled by tuning the length and packing density of VA-CNTs, have been produced [81–83] and investigated as ideal electrode materials for advanced supercapacitors [84–88]. By intercalated growth of VA-CNTs into thermally-expanded highly ordered pyrolytic graphite (HOPG), a 3D pillared VA-CNT/graphene architecture was

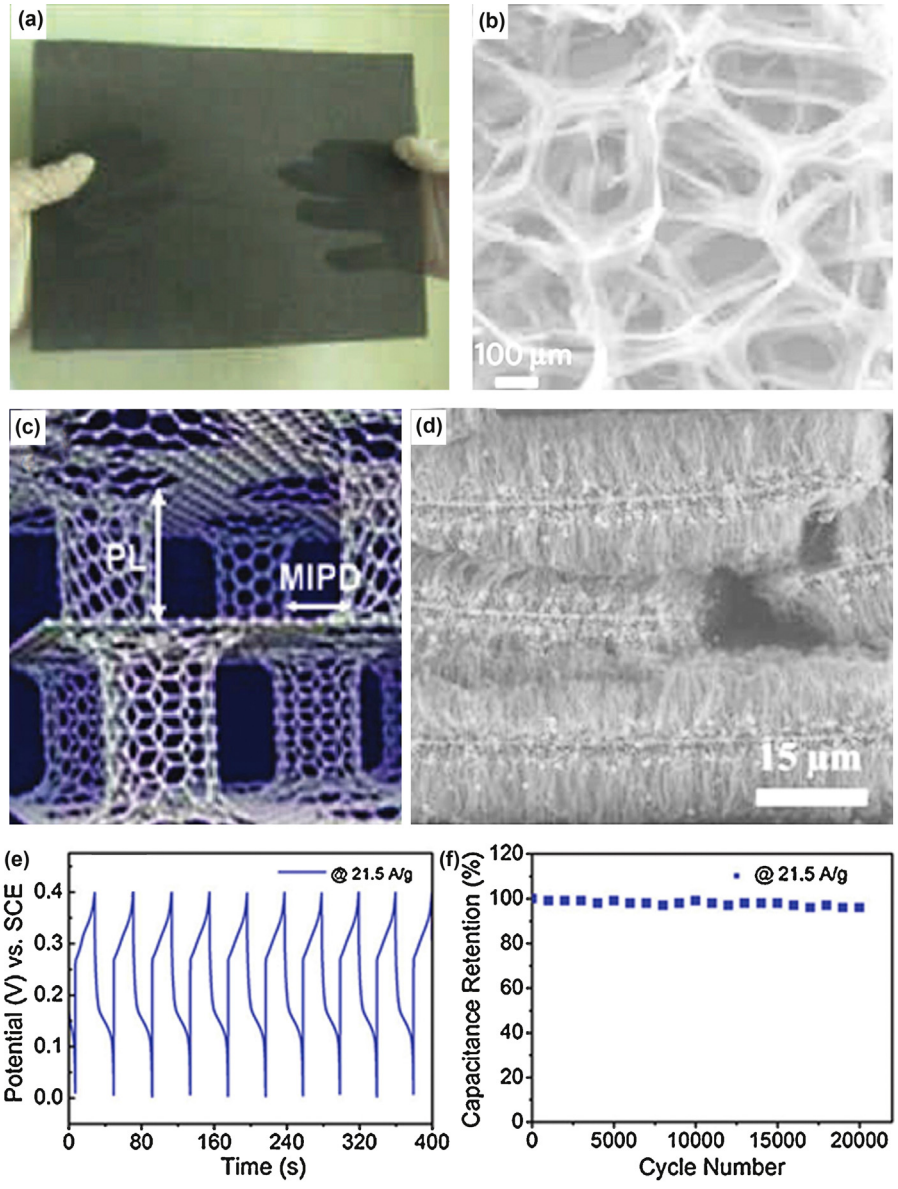

FIGURE 5

Structure of graphene foam, 3D pillared VA-CNT/graphene architecture and the electrochemical properties of its composite with $Ni(OH)_2$. (a) Photograph of a 17 cm × 22 cm free-standing graphene foam. (b) SEM image of a graphene foam [76]. Reprinted from Ref. [76] with permission. Copyright 2011, Nature Publishing Group. (c) Schematic diagram of a 3D pillared VA-CNT/graphene nanostructure. (d) Typical SEM images of the 3D pillared VA-CNT/graphene architectures. (e) Galvanostatic charge and discharge curves for the $Ni(OH)_2$-coated VA-CNT/graphene electrode at a current density of 21.5 A/g. (f) Dependency of the specific capacitance versus cycle number for the $Ni(OH)_2$-coated VA-CNT/graphene electrode at a galvanostatic charge and discharge current density of 21.5 A g^{-1} [89]. Reprinted from Ref. [89] with permission. Copyright 2009, American Chemical Society.

created (Fig. 5c,d) [89], which showed a specific capacitance of about 110 F g^{-1} in an electrical double layer supercapacitor. The resulting 3D pillared structure hybridized with nickel hydroxide coating showed a high specific capacitance (1065 F g^{-1}, Fig. 5e) with a remarkable rate capability and excellent long-term electrochemical stability – only 4% capacity loss after 20,000 charge–discharge cycles (Fig. 5f) [89].

The value of 1065 F g^{-1} is about 10 times that of the high-surface-area activated carbons (<100 F g^{-1}) [90] and within the range of 953–1335 F g^{-1} for graphene-supported single-crystalline nickel hydroxide hexagonal nanoplates [91]. In the 3D hierarchical structure, VA-CNTs can act as not only mechanical supports for the graphene layers but also good conductive paths for electrons and ions, and hence the high capacitance and excellent rate capability.

High-performance supercapacitors with novel structures

As discussed above, significant progress has been achieved with conventional supercapacitors based on liquid electrolytes. However, they cannot satisfy the requirements for certain specific applications, including portable, transparent and wearable electronics. In this regard, recent work on the development of lightweight, flexible, stretchable (Fig. 6a–c) [10–12] and/or transparent (Fig. 6d,e) [8,9] supercapacitors with novel structures (e.g. all-solid [6,7], fiber-shaped [13–15]; Fig. 6f–h) has attracted a great deal of attention. Highly-stretchable supercapacitors based on buckled SWNT macrofilm electrodes have also been developed by coating a thin SWNT film onto a pre-strained elastomeric substrate (polydimethylsiloxane, PDMS) and followed by relaxation of the pre-strained substrate (Fig. 6a) [11]. Even when these supercapacitors

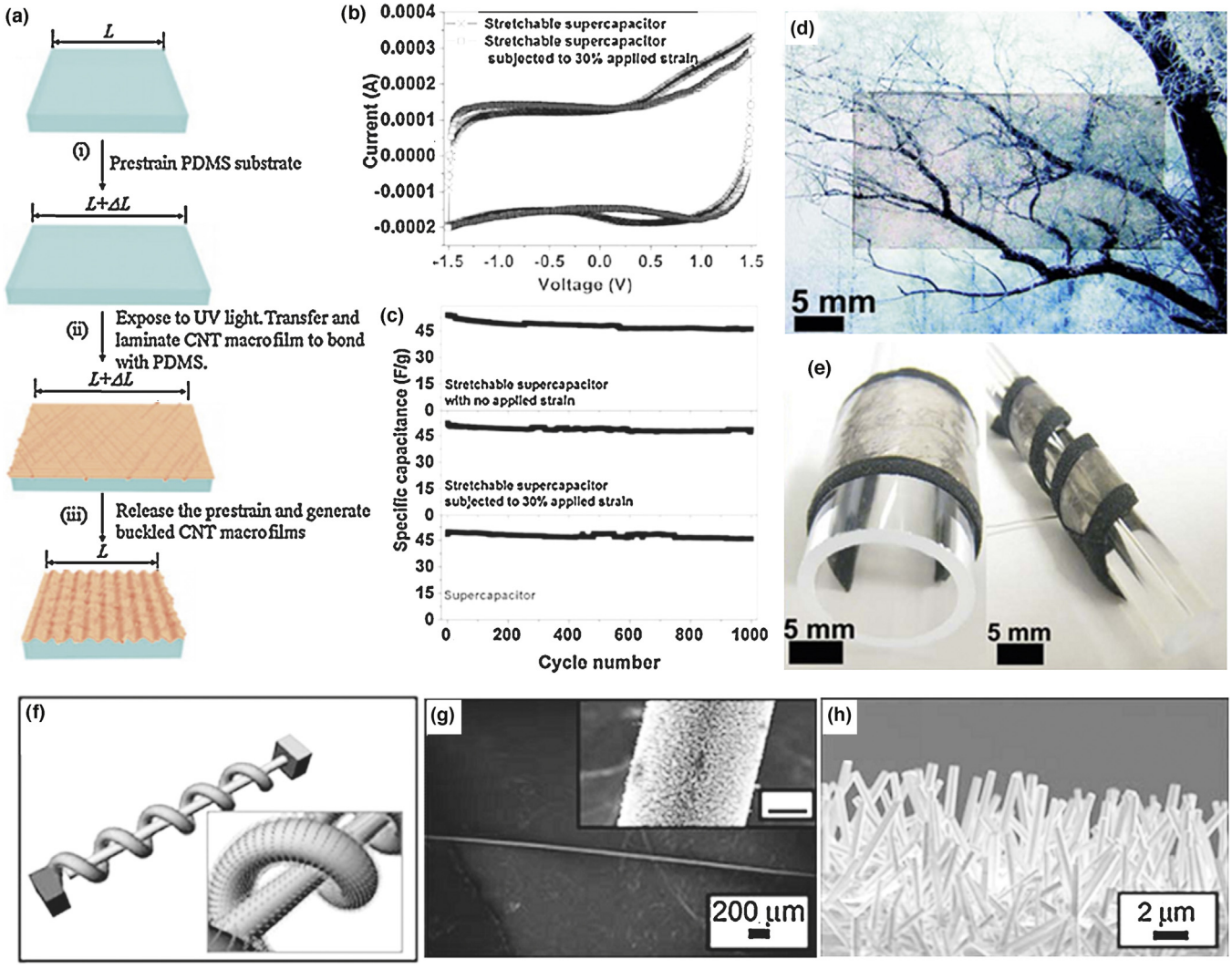

FIGURE 6

Supercapacitors with novel structures and their electrochemical performances: (a) Schematical illustration of the fabrication steps of a buckled SWNT macrofilm on an elastomeric PDMS substrate for stretchable supercapacitor. (b) Cyclic voltammograms of the stretchable supercapacitors measured at scan rates of 100 mV s^{-1}. (c) Long charge–discharge cycling at a constant current density of 1 A g^{-1} demonstrates the stability of the stretchable supercapacitor under 0 and 30% applied tensile strain [10]. Reprinted from Ref. [10] with permission. Copyright 2009, John Wiley and Sons. (d,e) Optical pictures demonstrating transparent (d) and flexible (e) natures of the supercapacitors [8]. Reprinted from Ref. [8] with permission. Copyright 2012, Nature Publishing Group. (f) Schematically illustration of a fiber-based supercapacitor. (g) Low-resolution SEM image of a Kevlar fiber covered with ZnO nanowire arrays. (Inset) A close-up view (scale bar: 10 μm). (h) Higher-magnification SEM image of the plastic wire, showing arrays of NWs [13]. Reprinted from Ref. [13] with permission. Copyright 2012, John Wiley and Sons.

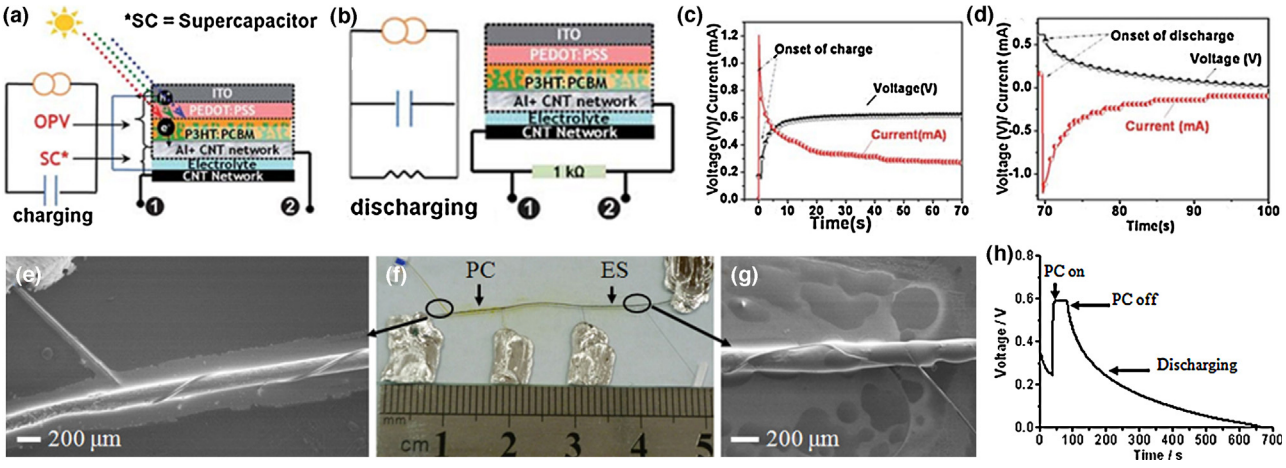

FIGURE 7

Structures and properties of integrated self-powering devices in planar and fiber forms. (a,b) Schematic and circuit illustrations of a PSC during the charging (a) and discharging (b) process. (c,d) The voltage and current profiles versus time for the charging (c) and discharging (d) process of a PSC [95]. Reprinted from Ref. [95] with permission. Copyright 2011, The Royal Society of Chemistry. (e) Photograph of a typical integrated wire-shaped device consisting of photoelectric conversion (PC) and energy storage (ES). (f) SEM image of the end PC part. (g) SEM image of the end ES part. (h) A typical photocharging–discharging curve of the integrated energy wire. The discharging current is 0.1 μA [98]. Reprinted from Ref. [98] with permission. Copyright 2012, John Wiley and Sons.

were stretched up to 30% stains, their electrochemical properties and stabilities remained almost unchanged with respect to the pristine state (Fig. 6b,c). By extension, stretchable electrodes based on graphene or aligned CNT films should be potential candidates for stretchable supercapacitors with a high efficiency [92,93], which can be used as the energy source for stretchable electronics. On the other hand, supercapacitors with high optical transparency (Fig. 6d,e) are useful for personal electronics and energy windows as power sources; they are also crucial components for many other power-integrated devices (e.g. self-powered light-emitting diodes, vide infra). Recently, supercapacitors in a fiber form (Fig. 6f–h) have been demonstrated to show many unique advantages, including being lightweight, wearable and flexible, for use as power sources by integrating them into clothing, bags and other textiles [13–15]. Specific capacitance as high as 38 mF cm^{-2} has been achieved for a fiber-shaped supercapacitor based on the CNT/PANI composite fiber electrodes [15].

Integrated self-powering systems

Self-powering systems with integrated energy conversion (e.g. solar cells) and storage (e.g. supercapacitors) devices have recently attracted more and more attention [94–96]. Using an SWNT network as the integration platform (Fig. 7a,b), for instance, a printable all-solid integrated device consisting of a polymer solar cell (PSC) and a supercapacitor has been developed [95]. The supercapacitor charged when the integrated device was under an illumination of 100 mW cm^{-1}, whereas discharging took place once the light source was switched off and the device was connected to a resistor as a load (Fig. 7a,b). Fig. 7c,d shows the voltage and current profiles versus time of the integrated system during the charging and discharging process, respectively, with a capacitance of 28 F g^{-1} [95]. Integrated devices containing an energy conversion unit and a supercapacitor in a single wire have also been devised for wearable electronics [97,98]. Specifically, Fig. 7e–g shows an integrated self-powering energy wire, consisting of a wire-shaped dye-sensitized solar cell (DSSC) and a supercapacitor both based on an aligned CNT fiber and modified titanium wire as the two electrodes, for simultaneous energy conversion and storage [98]. The supercapacitor in this integrated device can be rapidly charged to a voltage (Fig. 7h) close to the open-circuit voltage of the DSSC upon light irradiation. The entire energy conversion and storage efficiency up to 1.5% was obtained by multiplying the energy conversion efficiency of the solar cell part and the energy storage efficiency of the storage part. We anticipate considerable technical challenges ahead but also believe many more developments will be made over the next few years to advance the fiber-shaped integrated self-powering systems for wearable electronic applications.

Concluding remarks

With global energy consumption and CO_2 emissions increasing exponentially, it is crucial to develop clean and renewable energy systems and advanced energy storage devices. Nanotechnology has opened up new frontiers in materials science and engineering to meet this challenge by creating new materials and technologies for efficient energy conversion and storage. Of particular interest, carbon nanomaterials (e.g. CNTs and graphene) have been shown to be attractive for advanced energy storage applications. Recent research and development clearly indicate that high-performance supercapacitors can be prepared by using electrodes based on vertically-aligned CNTs with opened tips, graphene sheets with tunable through-thickness π–π stacking interactions and/or edge functionalities, and 3D pillared graphene-carbon nanotube networks. Their performance can be further enhanced by coating with conductive polymers and/or metal oxide to introduce pseudocapacitance. However, it is still challenging to further improve the performance of supercapacitors based on carbon nanomaterials. On one hand, the aggregation of CNTs and/or graphene materials tends to result in a loss of surface area, and hence inferior device performance. Carbon nanomaterials with various 3D architectures (such as CNT arrays, graphene foams, and 3D pillared VA-CNT/graphene networks), along with the 2D graphene sheet transferred onto a crumpled structure [99,100], have been developed to

prevent the aggregation. On the other hand, the relatively high cost compared to commercial mesoporous and/or activated carbon is another challenge for carbon nanomaterials to be scaled up for practical application in supercapacitors. Therefore, it is highly desirable to develop carbon nanomaterials with high charge capacity at a low cost (e.g. by ball milling).

For potential applications in portable and wearable optoelectronics, conventional supercapacitors are too heavy and bulky. To address these challenges, a few optically transparent, mechanically stretchable, and/or wearable wire-shaped supercapacitors have been developed based on limited electrode materials. The wire-shaped supercapacitors and the integrated self-powering systems play important roles in the development of flexible wearable optoelectronics. Aligned CNTs and/or graphene films with high transparency, stretchability, and charge mobility are promising electrodes for transparent, flexible, and/or stretchable supercapacitors, although it is still in the initial research stage. Continued research efforts in this embryonic field could give birth to a flourishing area of supercapacitor technologies.

Acknowledgement

The authors are grateful for financial support from AFOSR (FA9550-12-1-0037, FA-9550-12-1-0069 NSFC-NSF (DMR-1106160)).

References

1 M. Winter, R.J. Brodd, Chem. Rev. 104 (2004) 4245.
2 P. Simon, Y. Gogotsi, Nat. Mater. 7 (2008) 845.
3 M.D. Stoller, R.S. Ruoff, Energy Environ. Sci. 3 (2010) 1294.
4 L.L. Zhang, X. Zhao, Chem. Soc. Rev. 38 (2009) 2520.
5 W. Lu, L. Dai, in: J.M. Marulanda (Ed.), Carbon Nanotubes, In-Tech, 2010, pp. 563–589.
6 C. Meng, et al. Nano Lett. 10 (2010) 4025.
7 L. Yuan, et al. ACS Nano 6 (2012) 656.
8 H.Y. Jung, et al. Sci. Rep. 2 (2012) 773.
9 Z. Niu, et al. Small 9 (2013) 518.
10 C. Yu, et al. Adv. Mater. 21 (2009) 4793.
11 X. Li, et al. Nano Lett. 12 (2012) 6366.
12 Z. Niu, et al. Adv. Mater. 25 (7) (2013) 1058.
13 J. Bae, et al. Angew. Chem. Int. Ed. 50 (2011) 1683.
14 Z. Cai, et al. J. Mater. Chem. A 1 (2013) 258.
15 K. Wang, et al. Adv. Mater. 25 (2013) 1494.
16 L.L. Zhang, et al. J. Mater. Chem. 20 (2010) 5983.
17 K. Kierzek, et al. Electrochim. Acta 49 (2004) 515.
18 E. Raymundo-Pinero, et al. Carbon 44 (2006) 2498.
19 E. Raymundo-Pinero, et al. Adv. Mater. 18 (2006) 1877.
20 E. Frackowiak, F. Béguin, Carbon 39 (2001) 937.
21 B. Kastening, S. Spinzig, J. Electroanal. Chem. 214 (1986) 295.
22 S.T. Mayer, et al. J. Electrochem. Soc. 140 (1993) 446.
23 I. Tanahashi, et al. J. Electrochem. Soc. 137 (1990) 3052.
24 J. Chmiola, et al. Science 313 (2006) 1760.
25 J. Huang, et al. Angew. Chem. Int. Ed. 47 (2008) 520.
26 T.E. Rufford, et al. J. Phys. Chem. C 113 (2009) 1933.
27 A.K. Geim, K.S. Novoselov, Nat. Mater. 6 (2007) 183.
28 L. Dai, et al. Small 8 (2012) 1130.
29 S. Iijima, Nature 354 (1991) 56.
30 M. Cinke, et al. Chem. Phys. Lett. 365 (2002) 69.
31 C.M. Niu, et al. Appl. Phys. Lett. 70 (1997) 1480.
32 K.H. An, et al. Adv. Funct. Mater. 11 (2001) 387.
33 E. Frackowiak, et al. J. Power Sources 97–98 (2001) 822.
34 R.H. Baughman, et al. Science 297 (2002) 787.
35 D.N. Futaba, et al. Nat. Mater. 5 (2006) 987.
36 M. Kaempgen, et al. Nano Lett. 9 (2009) 1872.
37 A. Izadi-Najafabadi, et al. ACS Nano 5 (2011) 811.
38 C. Liu, et al. Nano Lett. 10 (2010) 4863.
39 M.D. Stoller, et al. Nano Lett. 8 (2008) 3498.
40 Y. Zhu, et al. Science 332 (2011) 1537.
41 K. Novoselov, et al. Nature 438 (2005) 197.
42 C. Lee, et al. Science 321 (2008) 385.
43 J.S. Wu, et al. Chem. Rev. 107 (2007) 718.
44 W. Lu, et al. J. Power Sources 189 (2009) 1270.
45 C.S. Du, et al. Nanotechnology 16 (2005) 350.
46 S.M. Huang, L.M. Dai, J. Phys. Chem. B 106 (2002) 3543.
47 H. Zhang, et al. Nano Lett. 8 (2008) 2664.
48 L.J. Gao, et al. Solid State Commun. 146 (2008) 380.
49 W. Lu, et al. ECS Trans. 6 (2008) 257.
50 H. Chen, et al. Mater. Sci. Eng. R: Rep. 70 (2010) 63.
51 A. Thess, et al. Science 273 (1996) 483.
52 B. Zheng, et al. Nano Lett. 2 (2002) 895.
53 L. Dai, et al. ChemPhysChem 4 (2003) 1150.
54 Y. Yan, et al. Small 3 (2007) 24.
55 L. Qu, L. Dai, J. Mater. Chem. 17 (2007) 3401.
56 Q.L. Chen, et al. Electrochim. Acta 49 (2004) 4157.
57 H. Zhang, et al. J. Electrochem. Soc. 155 (2008) K19.
58 F. Huang, et al. ChemSusChem 5 (2012) 888.
59 Y. Hu, et al. Electrochim. Acta 66 (2012) 279.
60 Y. Hou, et al. Nano Lett. 10 (2010) 2727.
61 Q. Wang, et al. Adv. Funct. Mater. 16 (2006) 2141.
62 Y.T. Kim, et al. J. Mater. Chem. 15 (2005) 4914.
63 R. Van Noorden, Nature 469 (2011) 14.
64 S. Park, R.S. Ruoff, Nat. Nanotechnol. 4 (2009) 217.
65 I.-Y. Jeon, et al. Proc. Natl. Acad. Sci. U. S. A. 109 (2012) 5588.
66 I.-Y. Jeon, et al. J. Am. Chem. Soc. 135 (2012) 1386.
67 L. Dai, Acc. Chem. Res. 46 (2013) 31.
68 J. Liu, et al. MRS Bull. 37 (2012) 1265.
69 J.L. Xia, et al. Nat. Nanotechnol. 4 (2009) 505.
70 C.G. Liu, et al. Nano Lett. 10 (2010) 4863.
71 M.F. El-Kady, et al. Science 335 (2012) 1326.
72 J. Xu, et al. ACS Nano 4 (2010) 5019.
73 Q. Wu, et al. ACS Nano 4 (2010) 1963.
74 X. Dong, et al. Carbon 50 (2012) 4865.
75 S.H. Lee, et al. Adv. Funct. Mater. 21 (2011) 1338.
76 Z.P. Chen, et al. Nat. Mater. 10 (2011) 424.
77 Y.H. Xue, et al. Angew. Chem. Int. Ed. 51 (2012) 12124.
78 X.H. Cao, et al. Small 7 (2011) 3163.
79 Y. Zhao, et al. Adv. Mater. 25 (2013) 591.
80 D. Yu, L. Dai, J. Phys. Chem. Lett. 1 (2010) 467.
81 G.K. Dimitrakakis, et al. Nano Lett. 8 (2008) 3166.
82 Y. Mao, J. Zhong, New J. Phys. 11 (2009) 093002.
83 V. Varshney, et al. ACS Nano 4 (2010) 1153.
84 Z. Fan, et al. Adv. Mater. 22 (2010) 3723.
85 R.K. Paul, et al. Small 6 (2010) 2309.
86 G.-P. Dai, et al. RSC Adv. 2 (2012) 8965.
87 V. Sridhar, et al. ACS Nano 6 (2012) 10562.
88 J. Lin, et al. Nano Lett. 13 (2013) 72.
89 F. Du, et al. Chem. Mater. 23 (2011) 4810.
90 O. Barbieri, et al. Carbon 43 (2005) 1303.
91 H.L. Wang, et al. J. Am. Chem. Soc. 132 (2010) 7472.
92 Y. Zhu, et al. Adv. Mater. 22 (2010) 3906.
93 K.S. Kim, et al. Nature 457 (2009) 706.
94 Z. Yang, et al. J. Mater. Chem. A 1 (2013) 954.
95 G. Wee, et al. Energy Environ. Sci. 4 (2) (2011) 413.
96 W. Guo, et al. Nano Lett. 12 (2012) 2520.
97 J. Bae, et al. Adv. Mater. 23 (2011) 3446.
98 T. Chen, et al. Angew. Chem. Int. Ed. 51 (2012) 11977.
99 J. Luo, et al. ACS Nano 5 (2011) 8943.
100 J. Luo, et al. ACS Nano 7 (2013) 1464.